Specific Recognition of Coiled Coils by Infrared Spectroscopy: Analysis of the Three Structural Domains of Type III Intermediate Filament Proteins

Thomas Heimburg,*[,‡,§] Juergen Schuenemann,[||] Klaus Weber,[||] and Norbert Geisler*[,||,⊥]

Max Planck Institute for Biophysical Chemistry, Departments of Spectroscopy and Biochemistry, D-37018 Göttingen, Federal Republic of Germany

Received July 12, 1995; Revised Manuscript Received November 13, 1995[⊗]

ABSTRACT: The central domain of cytoplasmic intermediate filament (IF) proteins from vertebrates contains some 310 residues and forms a double-stranded coiled coil (rod) with a length of about 46 nm. The flanking terminal domains show a high cell type specific variability both in sequence and in length. Using Fourier transform infrared (FTIR) spectroscopy we measured secondary structures of isolated domains of type III and IV IF proteins and of the soluble tetramers and the filaments formed by type III IF proteins. The amide I spectrum of the desmin rod is virtually identical to the spectra of other coiled-coil proteins such as tropomyosin and the myosin rod. All these double-stranded coiled coils reveal spectra distinctly different from classical α-helical spectra. The spectrum of coiled coils is a triplet of approximately equally strong bands. One band occurs at normal α-helix position, while the other two are found at lower wavenumbers. Theoretical aspects of these findings are discussed in the accompanying paper by W. C. Reisdorf and S. Krimm [(1996) *Biochemistry 35*, 1383−1386]. The amino-terminal head domain of desmin has a multicomponent spectrum with major fractions of β-sheet. The carboxy-terminal tail domains of desmin and the neurofilament proteins L and H, the latter in the phosphorylated and in the dephosphorylated forms, have very similar FTIR spectra, indicating mostly random structure. The spectrum of desmin type III protofilaments is very similar to the sum of the spectra of the three isolated domains. Polymerization into filaments seems to induce a small change in secondary structure.

The cytoplasmic intermediate filament (IF) proteins of vertebrates are conveniently divided into four major groups. Types I and II describe the epithelial keratins, which are the largest and most complex IF group. Type III covers vimentin, desmin, GFAP, and peripherin, which are able to form homopolymeric IF. The three neurofilament proteins NF-L, NF-M, and NF-H together with α-internexin form the type IV IF. All vertebrate cytoplasmic IF proteins have the same three-domain structure. The central domain of some 310 residues is essentially formed by α-helical segments with heptad repeats capable of forming a double-stranded coiled coil. This rod domain displays four helical stretches (helix 1A, 1B, 2A, and 2B) separated by short linkers and has a conserved heptad stutter in helix 2B. The rod is flanked by the amino-terminal head and carboxy-terminal tail domains. The nonhelical terminal domains of different IF types show striking differences in sequence and in length [reviewed in Steinert and Roop (1988) and in Fuchs and Weber (1994)]. Assembly of the dimeric coiled coils into IF proceeds via tetramers (protofilaments), and chemical cross-linking studies have defined major aspects of the filament lattice and drawn attention to a possible interaction between the ends of the rod, which are highly conserved in sequence (Geisler et al., 1992; Heins et al., 1993; Steinert et al., 1993a−c; Steinert & Parry, 1993).

Although the coiled-coils of the rod domain are the basic building block of the filaments, the presence of the amino-terminal head domain is required for filament assembly and maintenance (Geisler et al., 1982; Kaufmann et al., 1985; Traub & Vorgias, 1983). Head domains can be highly variable but are usually rather basic in charge. Particularly in type III IF proteins the head domains show a high amount of arginine residues and are also characterized by a wealth of glycine, aliphatic hydroxy amino acids, and to some extent the aromatic residues tyrosine and phenylalanine. Mutants of GFAP and vimentin point to two arginine-containing motif sequences required for filament assembly (Beuttenmüller et al., 1994; Herrmann et al., 1992; Traub et al., 1992; Hatzfeld et al., 1992; Ralton et al., 1994), and it is thought that the head domain may interact with coil 2 of the rod (Traub et al., 1992; Beuttenmüller et al., 1994). Although the secondary structure of the head domain of type III proteins has not been measured, prediction rules point to some β-structure (Shoeman et al., 1990).

The function of the tail domains in IF assembly and their structural organization is still a matter of debate. Although they do not seem necessary for filament formation by type III proteins *in vivo* and *in vitro*, they seem to influence lateral interactions and thus the filament diameter (Rogers et al., 1995; Herrmann et al., 1994; Eckelt et al., 1992; McCormick et al., 1993; Kouklis et al., 1991, 1993). The tail domains of type III proteins are around 55 residues in length and rather similar in sequence. In contrast the tail domains of type IV proteins range from 106 residues in porcine NF-L (Geisler et al., 1985) to 629 residues in human NF-H (Lees et al., 1988) and show unique sequence organizations. The tail domain of NF-L is very rich in glutamic acid (about 50%). The larger tail domains of NF-M and NF-H maintain a high content of glutamic acid and show in addition a large number

‡ Department of Spectroscopy.
§ Tel: +49 551 201 1491. Fax: +49 551 201 1501.
|| Department of Biochemistry.
⊥ Tel: +49 551 201 1486. Fax: +49 551 201 1578.
⊗ Abstract published in *Advance ACS Abstracts,* January 1, 1996.

0006-2960/96/0435-1375$12.00/0

of KSP phosphorylation sites arranged in repetitive sequences. Thus, the subdomain of the NF-H tail containing the repetitive phosphorylation sites accounts for two-thirds of the entire domain and provides some 50 phosphorylation sites. Most sites become phosphorylated during axonal transport. Phosphorylated and dephosphorylated tail domains of NF-H appear in the electron microscope as extended threads (Hisanaga & Hirokawa, 1989), but their secondary structure still poses a problem.

The three domains of the type III protein desmin can be readily obtained by limited proteolysis with chymotrypsin and by CNBr cleavage, respectively (Geisler et al., 1982). Thus, it seems possible to compare the secondary structural elements of the sum of the three domains with those of the tetrameric protofilaments and the intact filaments to decide whether IF assembly involves a detectable change in structure. Since circular dichroism is not suitable for the analysis of light-scattering structures such as polymerized IF, we turned to FTIR[1] spectroscopy to obtain insight into the structure of type III and IV filaments. The most important observation in this study is the finding that α-helices present in double-stranded coiled coils can be spectroscopically distinguished from normal α-helices by the amide I spectrum. This result is confirmed by the high similarity of the FTIR spectra of the rod domains of desmin and vimentin with those of the classical coiled-coil molecules tropomyosin and the myosin rod. In the accompanying paper, Reisdorf and Krimm show, on the basis of the crystal structure of tropomyosin, that the theoretically predicted amide I band shape has features similar to the spectra obtained experimentally.

MATERIALS AND METHODS

Proteins. Desmin was purified from chicked gizzard (Geisler & Weber, 1980). Desmin tail (residues 416−463) and rod (residues 70−415) were obtained by limited proteolysis of protofilaments with chymotrypsin (Geisler & Weber, 1982; Geisler et al., 1982). They were purified in 8 M urea buffer by chromatography on DEAE-cellulose. Desmin head (residues 1−88) produced by cleavage with CNBr was purified by chromatography on CM-cellulose (Geisler et al., 1982).

Recombinant hamster vimentin was kindly provided by Dr. Mechthild Hatzfeld. The four amino-terminal residues were changed due to the cloning procedure (Hatzfeld et al., 1992). Porcine neurofilament proteins L and H were isolated from spinal cord (Geisler & Weber, 1981). The tail domains obtained by limited proteolysis with chymotrypsin (Geisler et al., 1983, 1984) were purified by chromatography on DEAE-cellulose. The NF-H tail was dephosphorylated in 50 mM Tris/HCl buffer at pH 8.0 containing 1 mM $MgCl_2$ with *Escherichia coli* alkaline phosphatase (Sigma P4252). Separation of dephosphorylated tail and phosphatase was achieved by reversed-phase HPLC. The extent of the dephosphorylation was controlled by limited hydrolysis with HCl (6 N, 2 h, 110 °C) and pH 3.5 electrophoresis. No residual phosphoserine could be detected by staining with ninhydrine.

Bovine skeletal muscle tropomyosin was purified as described (Smillie, 1982). Bovine skeletal muscle myosin was prepared by standard procedures and mildly treated with chymotrypsin to obtain the myosin rod domain, which was purified as described (Fürst et al., 1992).

FTIR Spectroscopy. Before the FTIR spectra were recorded, all proteins were extensively dialyzed against D_2O buffers with at least two buffer changes (buffer volume, 20 mL; sample volume, 100 μL). Special care was taken that all traces of urea were removed by the dialysis. Desmin rod, desmin tail, and desmin head were measured in filament buffer (50 mM Tris/HCl, pD 7.5, 170 mM NaCl, and, if required, 1 mM 2-mercaptoethanol). Desmin protofilaments were measured in 10 mM sodium borate buffer at pD 9.0, 1 mM 2-mercaptoethanol. Desmin filaments were obtained by first dialyzing against protofilament buffer and then against filament buffer. Vimentin protofilaments and filaments were prepared in a similar manner. The neurofilament L and H tail domains were measured in filament buffer (see above). Myosin rod was in 50 mM sodium phosphate buffer, pD 7.0, containing 0.6 M KCl and 1 mM 2-mercaptoethanol. Tropomyosin was in 20 mM Tris/HCl, pD 7.5, supplemented with 170 mM NaCl and 1 mM 2-mercaptoethanol. Dialysis was at 4 °C, and protein concentrations were kept between 2 and 5 mg/mL.

FTIR spectroscopy was performed on a Bruker IFS25 spectrometer using a CaF_2 cell with a Teflon spacer (50 μm). The spectra (100 interferograms) were obtained in the range 400−4000 cm^{-1} with a spectral resolution of 2 cm^{-1}. The spectra were apodized with a triangular function before Fourier transformation. Fourier self-deconvolution was performed with software using routines provided by the laboratory of H. H. Mantsch/Ottawa (Kauppinen et al., 1981a,b). Resolution enhancement of unsmoothed spectra was performed using a triangular apodization function and line-narrowing factors between 1.5 and 2.5. The initial line width was assumed to be Lorentzian with a line width of 17 cm^{-1}. The spectral components of the resolution enhanced spectra were fitted with bands of Gaussian line shape (Byler & Susi, 1986). Spectra were recorded at room temperature. The deuterium exchange was found to be complete in each case.

RESULTS

Desmin Rod and Other Coiled-Coil Proteins. The FTIR spectrum of the desmin rod, a double-stranded coiled coil, was recorded in D_2O buffer after extensive dialysis. The shape of the spectrum (Figure 1) seemed at first to be incompatible with the high α-helical nature (>83%) earlier established by CD spectroscopy (Geisler et al., 1982). After deconvolution the FTIR spectrum shows three main peaks which become progressively more apparent at higher degrees of line narrowing (Figure 2a). While one peak occurs in the normal α-helical position (1653cm^{-1}), the other two (1640 and 1628 cm^{-1}) are found at considerably lower wavenumbers and are usually regarded as indicative of a random or β-sheet structure. Since less than 30% of the peak area was found in the traditional α-helix position, we explored the possibility that coiled-coil structure has an unusual amide I spectrum and turned to two proteins long established as classical double-stranded coiled coils.

Tropomyosin shows complete α-helix in CD spectroscopy (Pato et al., 1980), and its sequence displays the heptad repeats typical of coiled coils (McLachlan & Stewart, 1975).

[1] Abbreviations: CD, circular dichroism; FTIR, Fourier transform infrared spectroscopy.

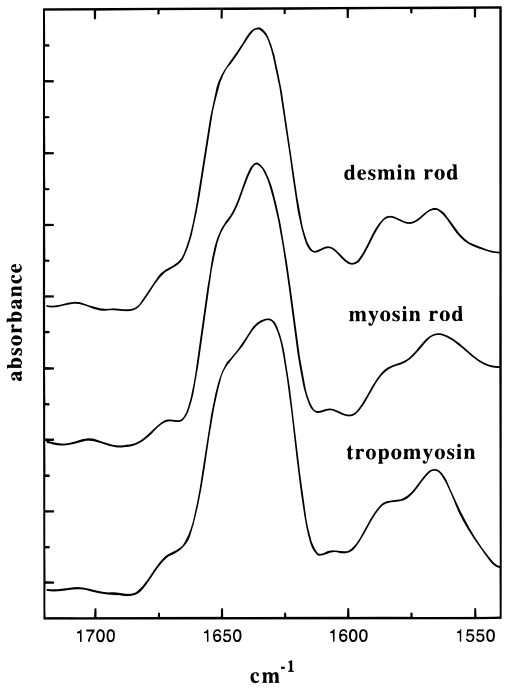

FIGURE 1: FTIR spectra of desmin rod, myosin rod, and tropomyosin. Note the striking spectral similarity of the different double-stranded coiled-coil proteins. Spectra are slightly enhanced in resolution ($K = 1.5$).

X-ray diffraction studies (Phillips et al., 1986; Whitby et al., 1992) show that the double-stranded coiled coil extends over nearly the entire molecular length. The rod domain of skeletal muscle myosin is well characterized as a coiled coil by the heptad repeats in its sequence (McLachlan & Karn, 1982) and its helical CD spectrum (Nozais & Dedret, 1993). FTIR spectra were taken in high-salt buffer to prevent head to tail polymerization of tropomyosin and paracrystal formation of the myosin rod. Figures 1 and 2 show that, consistent with a similar secondary structure, the spectra of desmin rod, myosin rod, and tropomyosin are remarkably similar.

Table 1: Band Analysis of Coiled-Coil Proteins

desmin rod		myosin rod		tropomyosin	
band position	area	band position	area	band position	area
1608.3	3.2	1606.7	2.5	1604.7	4.9
1628.3	24.2	1627.6	26.0	1626.2	24.4
1639.6	38.0	1638.9	40.7	1637.7	35.4
1652.9	27.0	1652.4	27.9	1651.5	27.6
1671.9	7.6	1672.7	2.9	1670.7	7.8

[a] Band analysis of slightly resolution enhanced spectra ($K = 1.5$) of the three different coiled-coil proteins (Figures 1 and 2) demonstrates the high similarity between the spectra. The predominant part of the overall band area is located at lower wavenumbers than the classical α-helix position at 1653 cm^{-1}.

Figure 2a,b shows the spectra of tropomyosin and the desmin rod at four different line-narrowing factors ($K = 1$, 1.5, 2, and 2.5). Figure 2c gives a detailed band analysis on a slightly deconvoluted spectrum of desmin rod using the peak maxima of the strongly deconvoluted spectrum (Figure 2a) and Gaussian line profiles (Byler & Susi, 1986). It was assumed that all bands have comparable widths which are consistent with the deconvolution procedure. The amide I band consists of at least three major bands positioned at approximately 1628, 1640, and 1653 cm^{-1}, respectively. Additional minor bands at higher and lower wavenumbers can be seen (Figures 1 and 2). The band position at 1653 cm^{-1} is typical of classical α-helix, while the bands at 1628 and 1640 cm^{-1} are usually assumed to indicate β-sheet and random coil [for review see Krimm and Bandekar (1986) and Surewicz et al. (1993)]. Table 1 summarizes the details of the band positions and areas of the individual bands for the three proteins in Figure 1 and demonstrates the striking spectral similarity of these double-stranded coiled coils. While the predominant part of the spectral weight of coiled-coil α-helices is found at wavenumbers below the classical α-helical position, significant shifts to lower wavenumbers have also been reported for stretched or distorted α-helices (Parrish & Blout, 1972; Trewhalla et al., 1989; Surewicz et al., 1993).

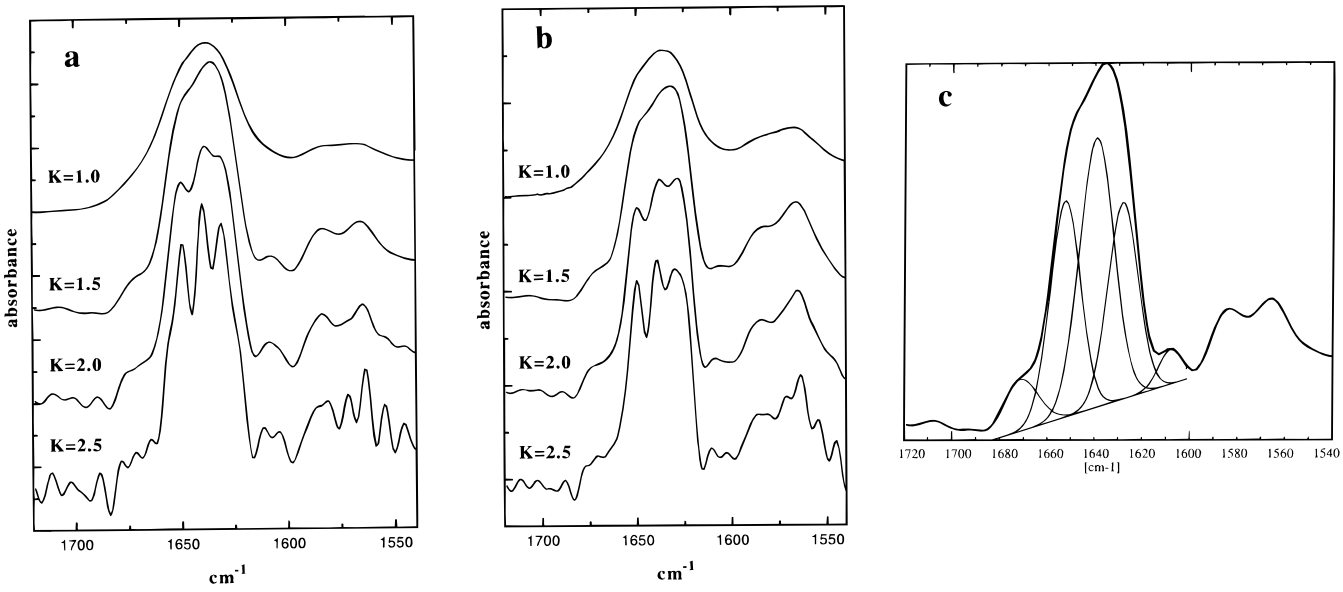

FIGURE 2: (a, b) Amide I spectra of desmin rod (a) and tropomyosin (b) at four different resolution enhancement factors: $K = 1.0$ (original spectrum), 1.5, 2.0, and 2.5. At the highest degree of band narrowing the central part of the spectra clearly shows three major components. (c) Band fit of the amide I band of desmin rod. Band positions were taken from the strongly deconvoluted spectrum in panel a. Note the presence of two strong bands at lower wavenumbers (1641 and 1632 cm^{-1}) in addition to the classical α-helix band (1652 cm^{-1}). The results of the band analysis are summarized in Table 1.

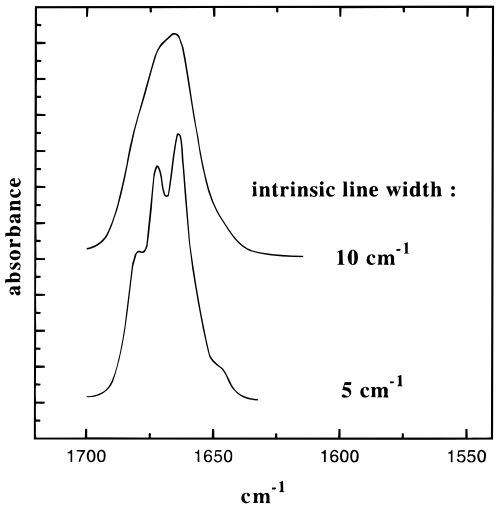

FIGURE 3: Coiled-coil spectrum of tropomyosin based on the theoretical predictions of Reisdorf and Krimm (see Figure 3b of the accompanying manuscript). Intrinsic linewidths of 10 and 5 cm^{-1} are used. The appearance of three major peaks is in close agreement with the experimental results (Figure 2). However, the band positions occur at higher wavenumbers than in the experimental curves. This difference may be due to double hydrogen bonding of amide carbonyl oxygens to the solvent water (see Discussion).

Using the X-ray structural information (Phillips et al., 1986; Whitby et al., 1992), Reisdorf and Krimm provide in the accompanying manuscript simulations of the tropomyosin infrared spectrum. One typical set of spectra from this analysis is reproduced with two different intrinsic line widths in Figure 3. These spectra reveal the typical three-line feature of coiled coils. However, in contrast to the experimental results (Figures 1 and 2) the simulations display the bands at significantly higher wavenumbers (Figure 3), probably because the hydrogen bonding of the experimental system is stronger than assumed in the simulation (see Discussion).

IF Tail Domains. Figure 4 compares the FTIR spectra of the tail domains of desmin and neurofilament proteins NF-L and NF-H. The NF-H tail was analyzed both in the isolated phosphorylated form and after enzymatic dephosphorylation. Although the tail domains of desmin and the neurofilament proteins differ distinctly in sequence (for references see introduction), the spectra are rather similar. They all display a pronounced maximum at about 1643 cm^{-1}. Figure 5 gives the band fitting for the desmin tail domain, and the results are summarized in Table 2. The peak corresponding to the band maximum contains approximately 50% of the overall intensity. Band shape and maximum are very similar to those of polylysine at pH 7 (Kleinschmidt, 1993), myelin basic protein (Surewicz et al., 1987), and apocytochrome *c* (Muga et al., 1991a), all of which have predominantly random-coil structure. Additionally, all IF-tails investigated here have been shown to be random-coil in circular dichroism experiments [Geisler et al. (1983) for the neurofilament tails, and our own unpublished results for the desmin tail]. Also, they do not show any indication of the 3−4 repeat pattern in the primary sequence typical for coiled coils. Thus, we assume that the tail domains of IF proteins also have a predominantly random-coil nature.

Desmin Head Domain. The head domain has a strong tendency to aggregate once urea is removed by dialysis. FTIR

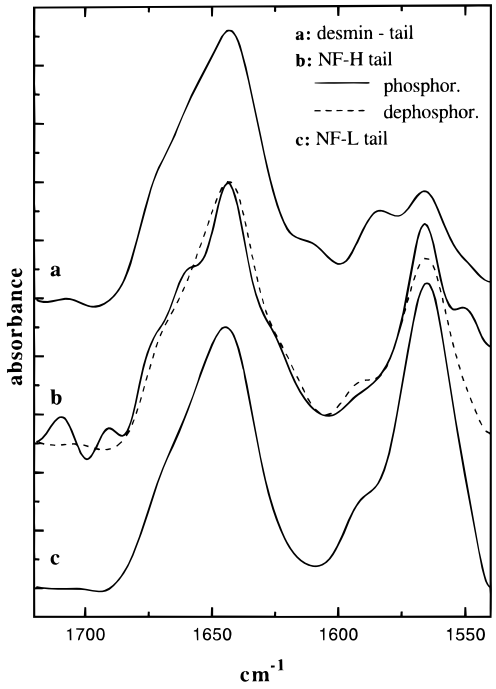

FIGURE 4: Amide I spectrum of tail domains of desmin and the neurofilament proteins NF-H and NF-L. The NF-H tail was measured in the phosphorylated and in the dephosphorylated form. Note the similar appearance of all spectra.

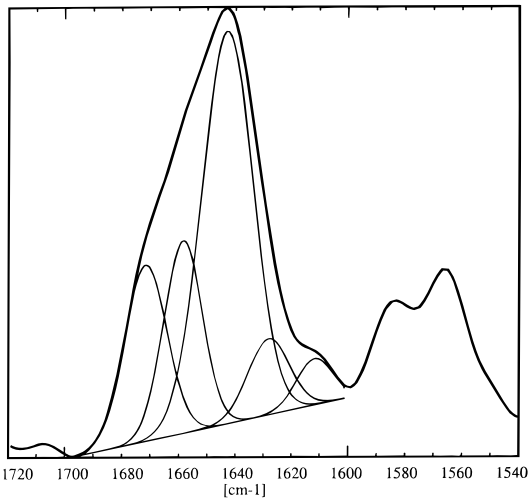

FIGURE 5: Band fit of a slightly resolution-enhanced spectrum ($K = 1.5$) of the desmin tail domain. The most prominent band is located at 1643 cm^{-1} and probably arises from random-coil structure (see Results). A summary of the band analysis is given in Table 2.

spectra had a low intensity and revealed water vapor distortions. Figure 6 shows the spectrum of the desmin head domain after slight deconvolution ($K = 1.5$). It was fitted with Gaussian line profiles using the parameters given in Table 2. The spectrum reveals a strong band at 1615 cm^{-1} and additional significant contributions in the region from 1672 to 1687 cm^{-1}. Such bands at very low wavenumbers in the amide I region often develop in aggregated or denatured proteins and have been attributed to intermolecular contacts of extended chain segments (Muga et al., 1991b; Heimburg & Marsh, 1993). If one additionally assigns the 1628 cm^{-1} band to β-sheet or extended chains, then roughly 70% of the overall band area belongs to this secondary structure. We therefore assigned these bands to antiparallel β-sheet structure [see Krimm and Bandekar (1986)]. Due

Table 2: Band Analysis of the Terminal Domains of IF Proteins[a]

desmin tail		neurofilament NF-H, tail phosphorylated		neurofilament NF-H, tail dephosphorylated		neurofilament NF-L, tail		desmin head	
band position	area	band position	area	band position	area	band position	area	band position	area
1611.8	4.2	1614.7	0.8					1615.0	27.6
1628.3	8.0	1627.3	15.5	1622.5	11.0	1625.4	4.1	1628.3	16.6
1643.3	50.5	1644.0	42.0	1643.0	56.7	1643.1	57.2	1642.1	18.2
1658.9	18.5	1661.4	28.1	1659.3	19.4	1656.4	16.7	1656.2	13.2
1672.1	18.7	1675.4	10.6	1671.8	12.9	1668.4	19.4	1672.3	15.9
								1686.9	8.5

[a] Band analysis of slightly resolution enhanced spectra ($K = 1.5$) of the tail domains of desmin and the two neurofilament proteins NF-L and NF-H (see Figures 4 and 5) and of the desmin head domain (Figure 6). The similarity of the band profiles in Figure 4 is reflected in the band areas. About 50% of the total band area is concentrated in a line at approximately 1643 cm^{-1}, which presumably corresponds to a random-coil configuration of the tail domains. Significant parts of the spectral area of the desmin head domain are concentrated in the outer wings of the amide I band. They seem to correspond to an antiparallel β-sheet configuration (see text for details).

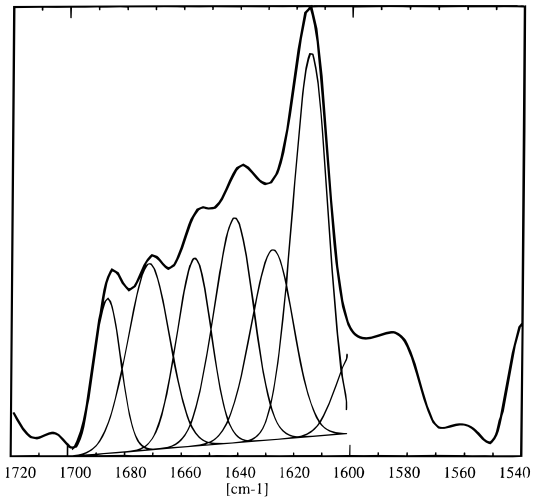

FIGURE 6: Band fit of a slightly resolution-enhanced spectrum ($K = 1.5$) of the desmin head domain. The main components are located in the outer wings of the amide I band and probably arise to a large degree from antiparallel β-sheet structure (see Results). A summary of the band analysis is given in Table 2.

to the ambiguity of the assignment of the random coil and the α-bands described above, we did not attempt to assign the two central bands (see Figure 6 and Table 2), which together account for approximately 30% of the overall area.

Protofilaments and Filaments of Type III IF Proteins. Protofilaments of desmin and vimentin revealed FTIR spectra very similar to those of the desmin rod (Figures 7 and 8). Figure 7 shows the slightly deconvoluted spectrum of desmin protofilaments and the spectra of the three individual domains: head, rod, and tail. The dotted line corresponding to the sum of the three domains is in good agreement with the spectrum of the protofilaments. Thus, the secondary structure of the domains present in the intact molecules is retained in the isolated individual domains. Interestingly, the β-sheet band at lower wavenumbers of the desmin head domain, which may be due to aggregation (see above), is also seen as a shoulder in the spectrum of desmin protofilaments.

When solutions of desmin or vimentin protofilaments are dialyzed against buffer 0.17 M in NaCl, a rather stiff gel is formed due to the polymerization into filaments. Figure 8 compares the spectra of protofilaments and filaments of desmin and vimentin. The spectra of the two protofilaments and the two filaments are very similar. Although the overall spectral shape is maintained when protofilaments are converted into filaments, there is a small change in the spectra.

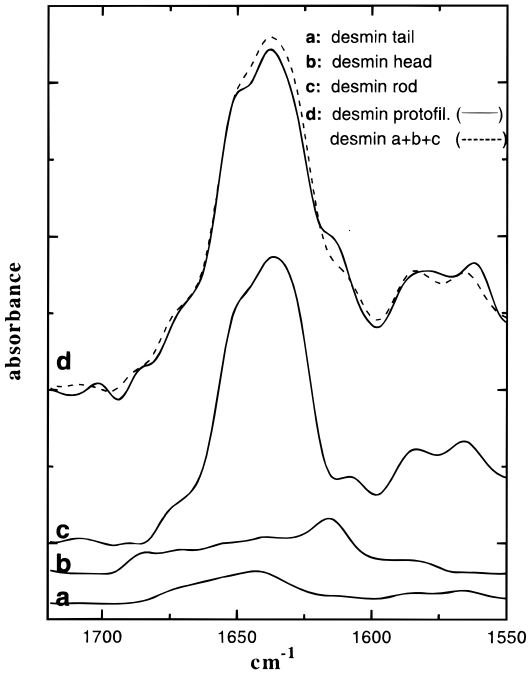

FIGURE 7: FTIR spectra of desmin protofilaments. Curve d gives the measured spectrum of the protofilaments (—) in comparison to the curve obtained by superposition of the spectra of the three individual domains (- - -). The three single-domain spectra are shown below: tail domain (curve a, compare Figure 5), head domain (curve b, compare Figure 6), and rod domain (curve c, compare Figure 2a). The spectra are displayed with areas corresponding to the total number of amino acid residues of the individual domain components. The relative percentages are 19% (head domain), 10% (tail domain), and 75% (rod domain). The sum of 104% arises from an 18-residue overlap between the head domain and the chymotryptic rod domain. All spectra are slightly resolution enhanced ($K = 1.5$).

It results in a broadening and slight repositioning of the bands in the filament samples. Thus, filament formation from protofilaments seems to involve small structural changes.

DISCUSSION

Coiled-Coil Proteins Have a Unique FTIR Spectrum. Here we have shown that three double-stranded coiled-coil proteins, tropomyosin, myosin rod, and desmin rod, have remarkably similar FTIR spectra, which are characterized by three major bands at 1652−1653, 1638−1640, and 1626−1628 cm^{-1}, respectively (Figures 1 and 2 and Table 1). While the former band occupies a classical α-helical position, the latter two are clearly shifted to lower wavenumbers. For

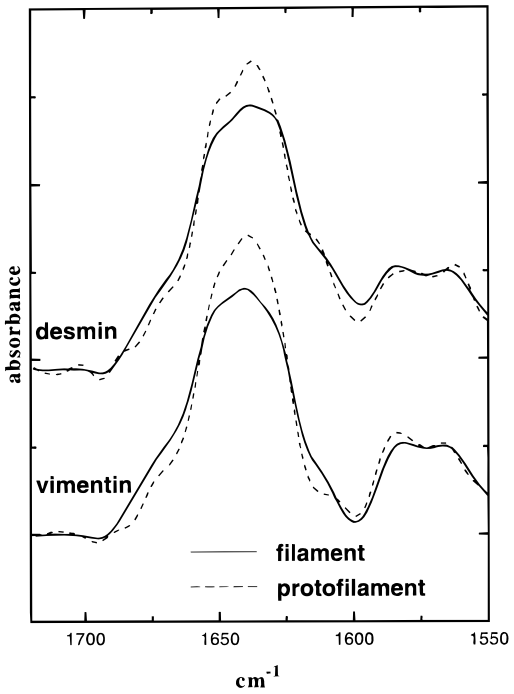

FIGURE 8: Comparison of protofilaments and filaments of desmin and vimentin. Protofilament- and filament spectra were normalized using the areas of the aspartic and glutamic acid carbonyls. Filament formation of both type III IF proteins seems to be accompanied by a small change in spectra (see text).

the following reasons all three major bands can be assigned to α-helical structure. All three proteins reveal the consecutive heptad patterns of coiled coils and are highly α-helical in CD analysis. The electron microscopical length of the rod-like molecules approaches the length calculated for coiled coils. Finally, in the case of tropomyosin, documentation of the coiled coil has been obtained by X-ray analysis (Phillips et al., 1986; Whitby et al., 1992). Thus, the three-band pattern can be considered as a spectral fingerprint of double-stranded coiled coils. As expected, we have recently also observed this spectrum in mollusc paramyosin, another coiled-coil protein (our unpublished results).

A possible explanation for two α-helical bands at lower wavenumbers comes from the structure of coiled-coil proteins. Their repeating pattern of hydrophobic amino acids at a frequency of 3.5 gives rise to the typical consecutive heptads. The two α-helices are coiled around each other along the hydrophobic seam provided by the hydrophobic residues in positions *a* and *d* of the heptads. Within this repeat pattern two consecutive amino acids experience different stretches due to the effect of the superhelix on the hydrogen bond distances. Parrish and Blout (1972) discussed the possibility of distorted α-helices in which the carbonyl oxygens are bent outward, resulting in dual or bifurcated hydrogen bonds between the carbonyl oxygen and an amide proton as well as a solvent molecule. This arrangement may result in a net gain of hydrogen-bonding strength and consequently in a band shift to lower wavenumbers (Tonge & Carey, 1992). In the accompanying manuscript, Reisdorf and Krimm have calculated the amide spectrum on the basis of the structural parameters provided by the X-ray data of tropomyosin. One typical set of their simulations is shown in Figure 3. While this approach leads nicely to the typical three-band pattern observed experimentally, the bands appear at considerably higher wavenumbers. Reisdorf and Krimm (1996) also argue that a shift to lower frequency should result due to additional hydrogen bonding of the solvent accessible backbone CO groups to water. If these views are correct, the spectra of coiled coils should be rather sensitive to solvents of different hydrogen-bonding capacity. As Reisdorf and Krimm point out (see accompanying paper), there is no doubt that one could simulate the experimental band positions by assuming stronger hydrogen bonding than in classical α-helices. Thus, they do not attempt to fit the theoretical spectra to the experimental curve. The difference of the spectral position of the calculated and experimental curves therefore suggests that hydrogen bonding is stronger in the coiled coil than in classical α-helices.

FTIR Spectra of the Terminal Domains. Although the tail domains of desmin and the neurofilament proteins NF-L and NF-H differ strikingly in sequence (for references see introduction), their FTIR spectra are rather similar (Figure 4 and Table 2), and the spectrum of the highly phosphorylated NF-H tail is not influenced by enzymatic dephosphorylation. Although two bands (at ∼1643 and 1627 cm^{-1}) of the tail spectra are at roughly similar positions as in the coiled-coil spectra, their relative band areas are quite different. Thus, the spectra of the coiled-coil proteins and the tail domains are distinctly different (compare Tables 1 and 2). While β-sheet structure is usually well defined in infrared spectra, it is sometimes difficult to distinguish between α-helical and random-coil contributions. Theoretical considerations and direct measurements usually place α-helical bands of deuterated polypeptides between 1650 and 1655 cm^{-1} (Krimm & Bandekar, 1986; Surewicz et al., 1993), but in some cases such as distorted helices (Parrish & Blout, 1972; Trewhalla et al., 1991) or very short helical segments (Reisdorf & Krimm, 1994) lower wavenumbers have been observed. The coiled-coil proteins analyzed in this study (see above) provide an additional example of band shift. Recently, the α-helical band of calcitonin was empirically assigned to 1637 cm^{-1} (Bauer et al., 1994) and in alanine-based peptides the helical band occurs in the range between 1632 and 1635 cm^{-1} (Matinez & Milhauser, 1995). One possible explanation for the shift of α-helical bands toward lower wavenumbers could be a distortion in the helices as discussed above. Random coiled-coil bands are usually assigned to the region 1640−1646 cm^{-1} (Surewicz et al., 1987; Chirgadze et al., 1973; Muga et al., 1991a), but recently a random-coil band was also placed at 1653 cm^{-1} (Bauer et al., 1994). These examples illustrate that difficulties can arise in distinguishing bands corresponding to α-helices and/or random coils. The sequence of the tail segments gives no indication of any repeat pattern typical for coiled-coil proteins. Also, CD spectra indicate only random structure [Geisler et al. (1983) and our unpublished results]. Our assignment of random-coil structure to the tail domains of IF proteins is mainly based on the spectral comparison with polylysine at pH 7, myelin basic protein, apocytochrome *c* (Kleinschmidt, 1993; Surewicz et al., 1987; Muga et al., 1991a), and our CD experiments.

The random-coil nature of the tail domains raises the question whether these domains on their own can renature properly after their isolation in urea solution. At least in the case of the desmin tail, this seems to be the case, since the FTIR spectrum of the polymerization competent desmin

protofilaments reflects the sum of the spectra of the three individual domains (Figure 7).

The head domain of desmin displays a major spectral component at 1615 cm^{-1} and smaller bands in the region 1672 to 1687 cm^{-1} (Figure 6). Antiparallel β-sheet typically shows a major band at approximately 1630 cm^{-1} and a minor band at 1672 cm^{-1}, but unusual shifts of the low-frequency band have been demonstrated in aggregated or denatured cytochrome *c* (Muga et al., 1991b; Heimburg & Marsh, 1993), avidin, and Na^+/K^+−ATPase (T. Heimburg, unpublished results). The head domain of desmin shows a strong tendency to aggregate. The FTIR spectrum indicates that a major part of the head domain consists of antiparallel β-sheet (∼70%, see results), where the low wavenumber of the major band may reflect the aggregation (Krimm & Bandekar, 1986). Since the polymerization competent desmin protofilaments show a spectrum corresponding to the sum of the three individual domains (Figure 7), the head domain in the protofilaments probably also displays β-sheet structure. Previous theoretical considerations of the head domain sequence of vimentin have also assumed the presence of a strong intramolecular antiparallel β-sheet (Shoeman et al., 1990).

The FTIR spectra of desmin and vimentin protofilaments show some change in shape upon polymerization into filaments (Figure 8). While the three-band pattern of the coiled coils is retained, some flattening or a slight repositioning of the bands appears. It remains to be seen whether these changes are at least in part related to a change in the hydrogen-bonding patterns. For instance, a number of the bifurcated hydrogen bonds involving also water molecules (see above) could be replaced by normal hydrogen bonds between neighboring double-stranded coiled coils and/or their dimers, i.e., the protofilaments. Indeed, a change in the hydrogen-bonding pattern of protofilaments and filaments could be an important aspect of the polymerization process.

CONCLUSIONS

FTIR spectroscopy is a valuable method for the investigation of secondary structure. Although most secondary structural features are found at distinct positions of the spectrum [for a review see Krimm and Bandekar (1986)], some special proteins show spectral bands at unusual positions. This holds for instance for the bands of α-helices, which are stretched and/or exposed to solvent. Thus, a certain ambiguity in the analysis of proteins of unknown structure can arise. On the other hand, such unusual features can also define the structure of a new class of related proteins. Here, we have shown that the double-stranded coiled proteins show a unique band pattern, clearly distinct from normal α-helical spectra. Assignment of coiled-coil structure has usually been based on the heptad repeat patterns seen directly in the sequence, a high α-helical content in CD analysis, and a rod-like molecular shape deduced by hydrodynamic properties and/or electron microscopy. Infrared spectroscopy now offers a direct spectroscopical identification.

ACKNOWLEDGMENT

We are grateful to Prof. S. Krimm for valuable discussions and for allowing us to include the theoretical results on tropomyosin in Figure 3 of this report.

REFERENCES

Bauer, H. H., Müller, M., Goette, J. Merkle, H. P., & Fringeli, U. P. (1994) *Biochemistry 33*, 12276−12282.
Beuttenmüller, M., Chen, M., Janetzko, A., Kühn, S., & Traub, P. (1994) *Exp. Cell. Res. 212*, 128−142.
Byler, D. M., & Susi, H. (1986) *Biopolymers 25*, 469−487.
Chirgadze,Y. N., Shestopalov, B. V., & Yu, S. (1973) *Biopolymers 12*, 1337−1351.
Eckelt, A., Herrmann, H., & Franke, W. W. (1992) *Eur. J. Cell Biol. 58*, 319−330.
Fuchs, E., & Weber, K. (1994) *Annu. Rev. Biochem. 63*, 345−382.
Fürst, D. O., Vinkemeier, U., & Weber, K. (1992) *J. Cell. Sci. 102*, 769−778.
Geisler, N., & Weber, K. (1980) *Eur. J. Biochem. 111*, 425−433.
Geisler, N., & Weber, K. (1981) *J. Mol. Biol. 151*, 565−571.
Geisler, N., & Weber, K. (1982) *EMBO J. 1*, 1649−1656.
Geisler, N., Kaufmann, E., & Weber, K. (1982) *Cell 30*, 277−286.
Geisler, N., Kaufmann, E., Fischer, S., Plessmann, U., & Weber, K. (1983) *EMBO J. 2*, 1295−1302.
Geisler, N., Fischer, S., Vandekerckhove, J., Plessmann, U., & Weber, K. (1984) *EMBO J. 3*, 2701−2706.
Geisler, N., Plessmann, U., & Weber, K. (1985) *FEBS Lett. 182*, 475−478.
Geisler, N., Schuenemann, J., & Weber, K. (1992) *Eur. J. Biochem. 206*, 841−852.
Goto, T., Tanaka, T., Nakamura, Y., & Takeda, M. (1994) *J. Cell. Sci. 107*, 1949−1957.
Hatzfeld, M., Dodemont, H., Plessmann, U., & Weber, K. (1992) *FEBS Lett. 302*, 239−242.
Heimburg, T., & Marsh, D. (1993) *Biophys. J. 65*, 2408−2417.
Heins, S., Wong, P. C., Müller, S., Goldie, K., Cleveland, D., & Aebi, U. (1993) *J. Cell Biol. 123*, 1517−1533.
Herrmann, H., Hofmann, I., & Franke, W. W. (1992) *J. Mol. Biol. 223*, 637−650.
Hisanaga, S., & Hirokawa, N. (1989) *J. Neurosci. 9*, 959−966.
Kaufmann, E., Weber, K., & Geisler, N. (1985) *J. Mol. Biol. 185*, 733−742.
Kauppinen, J. K., Moffat, D. J., & Mantsch, H. H. (1981a) *Appl. Spectrosc. 35*, 271−276.
Kauppinen, J. K., Moffat, D. J., Mantsch, H. H., & Cameron, D. G. (1981b) *Anal. Chem. 53*, 1454−1457.
Kleinschmidt, J. (1993) Ph.D. Thesis, University of Göttingen, Germany.
Kouklis, P. D., Papamarcabi, T., Merdes, A., & Georgatos, S. D. (1991) *J. Cell Biol. 114*, 773−786.
Kouklis, P. D., Hatzfeld, M., Brunkener, M., Weber, K., & Georgatos, S. D. (1993) *J. Cell Sci. 106*, 919−928.
Krimm, S., & Bandekar, J. (1986) *Adv. Protein Chem. 38*, 181−364.
Lees, J. F., Shneidman, P. S., Skuntz, S. F., Carden, M. J., & Lazzarini, R. A. (1988) *EMBO J. 7*, 1947−1955.
McCormick, M. B., Kouklis, P., Snyder, A., & Fuchs, E. (1993) *J. Cell Biol. 122*, 395−407.
McLachlan, A. D., & Karn, J. (1982) *Nature 299*, 226−231.
McLachlan, A. D., & Stewart, M. (1975) *J. Mol. Biol. 98*, 293−304.
Matinez, G., & Milhauser, G. (1995) *J. Struct. Biol. 114*, 23−27.
Muga, A., Mantsch, H. H., & Surewicz, W. K. (1991a) *Biochemistry 30*, 2629−2635.
Muga, A., Mantsch, H. H., & Surewicz, W. K. (1991b) *Biochemistry 30*, 7219−7224.
Nozais, M., & Bechet, J.-J. (1993) *Eur. J. Biochem. 218*, 1049−1055.
Parrish, J. R., & Blout, E. R. (1972) *Biopolymers 11*, 1001−1020.
Pato, M. D., Mak, A. S., & Smillie, L. B. (1980) *J. Biol. Chem. 256*, 593−601.
Phillips, G. N., Jr., Fillers, J. P., & Cohen, C. (1986) *J. Mol. Biol. 192*, 111−131.
Ralton, J. E., Lu, X., Hutcheson, A. M., & Quinlan, R. A. (1994) *J. Cell Sci. 107*, 1935−1948.
Reisdorf, W. C., & Krimm, S. (1994) *Biophys. J. 65*, A373.
Reisdorf, W. C., & Krimm, S. (1996) *Biochemistry 35*, 1383−1386.

Rogers, K. R., Eckelt, A., Nimmrich, V., Janssen, K. P., Schliwa, M., Herrmann, H., & Franke, W. W. (1995) *Eur. J. Cell Biol. 66*, 136−150.

Shoeman, R. L., Mothes, E., Kesselmeier, C., & Traub, P. (1990) *Cell Biol. Int. Rep. 14*, 583−594.

Smillie, L. B. (1982) *Methods Enzymol. 35*, 234−241.

Steinert, P. M., & Roop, D. R. (1988) *Annu. Rev. Biochem. 57*, 593−625.

Steinert, P. M., & Parry, D. A. D. (1993) *J. Biol. Chem. 268*, 2878−2887.

Steinert, P. M., Marekov, L. N., Fraser, R. D. B., & Parry, D. A. D. (1993a) *J. Mol. Biol. 230*, 436−452.

Steinert, P. M., Marekov, L. N., & Parry, D. A. D. (1993b) *J. Biol. Chem. 268*, 24916−24925.

Steinert, P. M., Marekov, L. N., & Parry, D. A. D. (1993c) *Biochemistry 32*, 10046−10056.

Surewicz, W. K., Moscarello, M. A., & Mantsch, H. H. (1987) *Biochemistry 26*, 3881−3886.

Surewicz, W. K., Mantsch, H. H., & Chapman, D. (1993) *Biochemistry 32*, 389−394.

Tonge, P. J., & Carey, P. R. (1992) *Biochemistry 31*, 9122−9125.

Traub, P., & Vorgias, C. E. (1983) *J. Cell Sci. 63*, 43−67.

Traub, P., Scherbarth, A., Wiegers, W., & Shoeman, R. L. (1992) *J. Cell Sci. 101*, 363−381.

Trewhella, J., Liddle, W. K., Heidorn, D. B., & Strynadka, N. (1989) *Biochemistry 28*, 1294−1301.

Whitby, F. G., Kent, H., Stewart, F., Stewart, M., Xie, X., Hatch, V., Cohen, C., & Phillips, G. N., Jr. (1992) *J. Mol. Biol. 227*, 441−452.

BI9515883